BJP BRITISH JOURNAL OF PHARMACOLOGY
BPS BRITISH PHARMACOLOGICAL SOCIETY

BJP British Journal of Pharmacology

DOI:10.1111/j.1476-5381.2010.00859.x
www.brjpharmacol.org

RESEARCH PAPER

Effect of the I_{to} activator NS5806 on cloned K_V4 channels depends on the accessory protein KChIP2

A Lundby[1], T Jespersen[1], N Schmitt[1], M Grunnet[1,2], S-P Olesen[1,2], JM Cordeiro[3] and K Calloe[1]

[1]*The Danish National Research Foundation Centre for Cardiac Arrhythmia, Department of Biomedical Sciences, University of Copenhagen, Copenhagen, Denmark,* [2]*NeuroSearch A/S, Ballerup, Denmark, and* [3]*Masonic Medical Research Laboratory, Utica, NY, USA*

Correspondence
Kirstine Calloe, Danish National Research Foundation Centre for Cardiac Arrhythmia (DARC), Department of Biomedical Sciences 12.5.10, University of Copenhagen, Blegdamsvej 3, DK-2200 Copenhagen N, Denmark. E-mail: kirstinec@mfi.ku.dk

Keywords
I_{to}; transient outward potassium current; $K_V4.3$; $K_V1.4$; KChIP2; DPP6; KCNE; NS5806

Received
19 August 2009
Revised
9 February 2010
Accepted
22 March 2010

BACKGROUND AND PURPOSE

The compound NS5806 increases the transient outward current (I_{to}) in canine ventricular cardiomyocytes and slows current decay. In human and canine ventricle, I_{to} is thought to be mediated by $K_V4.3$ and various ancillary proteins, yet, the exact subunit composition of I_{to} channels is still debated. Here we characterize the effect of NS5806 on heterologously expressed putative I_{to} channel subunits and other potassium channels.

EXPERIMENTAL APPROACH

Cloned K_V4 channels were co-expressed with KChIP2, DPP6, DPP10, KCNE2, KCNE3 and $K_V1.4$ in *Xenopus laevis* oocytes or CHO-K1 cells.

KEY RESULTS

NS5806 increased $K_V4.3$/KChIP2 peak current amplitudes with an EC_{50} of 5.3 ± 1.5μM and significantly slowed current decay. KCNE2, KCNE3, DPP6 and DPP10 modulated $K_V4.3$ currents and the response to NS5806, but current decay was slowed only in complexes containing KChIP2. The effect of NS5806 on $K_V4.2$ was similar to that on $K_V4.3$, and current decay was only slowed in presence of KChIP2. However, for $K_V4.1$, the slowing of current decay by NS5806 was independent of KChIP2. $K_V1.4$ was strongly inhibited by 10 μM NS5806 and $K_V1.5$ was inhibited to a smaller extent. Effects of NS5806 on kinetics of currents generated by $K_V4.3$/KChIP2/DPP6 with $K_V1.4$ in oocytes could reproduce those on cardiac I_{to} in canine ventricular myocytes. $K_V7.1$, $K_V11.1$ and $K_{ir}2$ currents were unaffected by NS5806.

CONCLUSION AND IMPLICATIONS

NS5806 modulated K_V4 channel gating depending on the presence of KChIP2, suggesting that NS5806 can potentially be used to address the molecular composition as well as the physiological role of cardiac I_{to}.

Abbreviations

CHO-K1, Chinese hamster ovary cells; DPP, dipeptidyl-peptidase; I_A, A-type potassium current; I_{to}, transient outward potassium current; KChIP2, K channel interacting protein 2

Introduction

Epi- and midmyocardial cells from larger mammals have a prominent phase 1 repolarization of the action potential due to the presence of a Ca^{2+}-independent transient outward potassium current (I_{to}). In human and canine hearts, I_{to} is principally mediated by the α-subunit $K_V4.3$, but other channels such as $K_V1.4$ may be involved (Dixon *et al.*, 1996; Akar *et al.*, 2004; channel nomenclature follows Alexander *et al.*, 2009). However, heterologously expressed $K_V4.3$ channels do not reproduce

the kinetics of native cardiac I_{to} and $K_V4.3$ has been demonstrated to assemble with various ancillary β-subunits in cardiac tissue; the most prominent of which is K Channel Interaction Protein 2 (KChIP2). KChIP2 belongs to a large family of cytosolic Ca^{2+} – sensing proteins that contain up to four putative Ca^{2+} binding EF-hands. KChIP2 increases $K_V4.3$ current density by facilitating trafficking, slowing inactivation and by accelerating recovery kinetics (An *et al.*, 2000). Interestingly, the expression of KChIP2 mRNA is more abundant in epi- and mid-myocardium than in endocardium and this differential expression of KChIP2 has been suggested to underlie the transmural I_{to} gradient (Rosati *et al.*, 2001; 2003; Calloe *et al.*, 2009b). Besides KChIP2, several other proteins expressed in ventricular tissue have been shown to interact with $K_V4.3$. Dipeptidyl-peptidase (DDP) 6 can facilitate $K_V4.3$ trafficking, accelerate $K_V4.3$ inactivation (Nadal *et al.*, 2003) and increase single channel conductance of $K_V4.2$ (Kaulin *et al.*, 2009). Co-expression of $K_V4.3$ with KChIP2 and DPP6 in heterologous systems results in currents with kinetics similar to those of I_{to} in human ventricular myocytes (Radicke *et al.*, 2005).

Members of the KCNE β-subunit family have been shown to modulate $K_V4.3$ currents (Zhang *et al.*, 2001; Lundby and Olesen, 2006; Radicke *et al.*, 2006). KCNE2 may be a promising candidate for the human I_{to} channel complex as co-expression of K_V4 channels with KCNE2 induced an overshoot of peak current during recovery from inactivation (Zhang *et al.*, 2001; Radicke *et al.*, 2006), comparable to that described for I_{to} in human epicardial myocytes (Wettwer *et al.*, 1994). However, other studies have shown that KCNE2 is expressed in low quantities in ventricular tissue compared with Purkinje tissue (Pourrier *et al.*, 2003) suggesting KCNE2 is important mainly in the conduction system of the heart (Sanguinetti and Tristani-Firouzi, 2006). KCNE3 has been shown to inhibit $K_V4.3$ currents (Lundby and Olesen, 2006) and mutations in KCNE3 resulting in less inhibition of $K_V4.3$ current have been linked to the Brugada syndrome (Delpón *et al.*, 2008) and atrial fibrillation (Lundby *et al.*, 2008). Furthermore, heterologously expressed $K_V4.3$ channels are modulated by $K_V\beta$, KChAP and $Na_V\beta$ accessory subunits (Deschenes and Tomaselli, 2002) but their physiological roles have yet to be determined.

K_V4 currents are selectively inhibited by several spider toxins that modify gating kinetics, including the *Heteropoda venatoria* toxins (Sanguinetti *et al.*, 1997) HpTX2 (Zarayskiy *et al.*, 2005) and HpTX3 (Brahmajothi *et al.*, 1999), the *Phrixotrichus auratus* toxins PaTx1 and PaTx2 (Diochot *et al.*, 1999) and the *Theraphosa leblondi* toxins TLx1-3 (Ebbinghaus *et al.*, 2004). In common with other A-type K_V channels, $K_V4.3$ is blocked by 4-aminopyridine (4-AP) in millimolar range concentrations (Wang *et al.*, 1995). I_{to} is blocked by several sodium channel blockers, including flecainide (Radicke *et al.*, 2008) and quinidine (Wang *et al.*, 1995), and several calcium channel blockers, including nifedipine (Hatano *et al.*, 2003; Bett *et al.*, 2006). We have recently added an I_{to} activator, NS5806, to this list of compounds affecting I_{to} and described the effect of NS5806 on canine ventricular wedge preparations (Calloe *et al.*, 2009a) as well as on native I_{to} in isolated cells from canine left ventricular epi-, mid- and endocardium (Calloe *et al.*, 2009b). We found that 10 μM NS5806 increased the magnitude of $I_{to,}$ slowed current decay, induced a negative shift in steady-state inactivation and accelerated recovery from inactivation for native I_{to}.

In the present study, we characterized the effects of NS5806 on heterologously expressed putative I_{to} channel subunits. NS5806 enhanced peak currents for all K_V4 channels and affected channel gating. In the presence of KChIP2, NS5806 slowed the decay of $K_V4.2$ and $K_V4.3$ currents significantly, whereas it had little effect in the absence of KChIP2. Co-expression of $K_V4.3$ with and without KChIP2 with DPP6, DPP10, KCNE2 or KCNE3 β-subunits corroborated that NS5806 only slowed current decay of channel complexes containing KChIP2. Besides the effects on K_V4 channels, NS5806 inhibited $K_V1.4$ and $K_V1.5$ mediated currents independently of the presence of KChIP2. Effects of NS5806 on currents generated by $K_V4.3$/KChIP2/DPP6 with $K_V1.4$ in oocytes could reproduce those on cardiac I_{to} in canine ventricular myocytes

Methods

NS5806

NS5806 (1-[2,4-dibromo-6-(1H-tetrazol-5-yl)-phenyl]-3-(3,5-bis-trifluoromethyl-phenyl)-urea) was synthesized at NeuroSearch A/S (Ballerup, Denmark) by reaction of 6-cyano-2,4-dibromoaniline with sodium azide to form the respective 2,4-dibromo-6-tetrazolylaniline, which was condensed with 3,5-bis-trifluoromethyl-phenylisocyanate to provide the final product, NS5806. NS5806 was dissolved in DMSO to give a concentrated stock solution of 30 mM. The final DMSO concentration never exceeded 0.1%, and at this concentration DMSO did not influence the electrical properties of the cells.

Molecular biology

α-subunits. cDNAs coding for human (h) Kv4.1 (NM_004979) and hKv4.2 (NM_012281) were a kind

gift from D. Isbrandt (U Hamburg, Germany). cDNA coding for hKv4.3 (short isoform, NM_172198) and hKv1.5 (NM_002234) were kindly provided by O. Pongs (U Hamburg, Germany). hKv4.3 cDNA was subcloned into the expression vector pXOOM, Kv1.5 was cloned into pXOON. hKv4.1 and hKv4.2 were PCR-amplified and cloned into the expression vector pGEM-HEJuel. cDNA encoding hKv1.4 (NM_002233) was amplified from EST HU_p940D11203D (ImaGenes, Berlin, Germany) and cloned into pGEM-HEJuel.

Ancillary subunits. hKChIP2.1 (NM_173192) was amplified from IMAGE clone 2430271 and subcloned into pXOOM. cDNA coding for hDPP6 iso 2 (NM_001936) and hDPP10 iso 1 (NM_020868) were kindly provided by E. Wettwer (TU Dresden, Germany), PCR-amplified and cloned into pGEM-HEJuel. KCNE2 (NM_172201) in pSGEM and hKCNE3 (NM_005472) in pXOOM have been described previously (Lundby and Olesen, 2006). All constructs were verified by sequencing.

Heterologous expression in Xenopus laevis oocytes

All animal care and experimental procedures were in accordance with Danish National Committee for Animal Studies guidelines. Female *Xenopus laevis* frogs were anesthetized (2 g·L^{-1} Tricaine; Sigma) and ovarian lobes cut off through a small abdominal incision. The oocytes were manually dissected into smaller groups and defolliculated using collagenase (Type 1, Sigma-Aldrich) for 1 h. Oocytes were kept in Kulori solution (mM); NaCl 90, KCl 4, $MgCl_2$ 1, $CaCl_2$ 1, HEPES 5, pH 7.4 with NaOH at 19°C for 24 h before injection of cRNA. cRNA was prepared from linearized plasmid DNA using the T7 mMessage mMachine kit (Ambion) according to the manufacturer's instructions. 50 nl containing 0.5 ng K_V4 cRNA and ancillary subunits added in a 1:1 molar ratio was injected using a Nanoject microinjector (Drummond Scientific, Broowell, PA, USA). $K_V4.3$/KChIP2 and $K_V1.4$ channels were co-expressed in a 1:1 current ratio corresponding to 0.15 ng $K_V4.3$ + 0.15 ng KChIP2 + 1.3 ng $K_V1.4$ pr oocyte. The oocytes were kept in Kulori solution at 19°C, which was changed daily and currents were recorded after 2 to 3 days.

Two-electrode voltage clamp

Recordings were at room temperature in Kulori solution using a two-electrode voltage-clamp amplifier (Dagan CA-1B; Chicago, IL, USA). Borosilicate glass recording electrodes (Module Ohm, Denmark) were fabricated using a DMZ-Universal Puller (Zeitz Instruments, Munich, Germany) and had a resistance of 0.5 to 1 MΩ when filled with 3 M KCl.

CHO-K1 cell culture and transfection

CHO-K1 cells were transiently transfected with $hK_V4.3$ (0.5 µg to a 25 cm^2 cell flask), hKChIP2.1, hDPP6 in a 1:3:3 molar ratio using Lipofectamine and Plus Reagent according to manufacturer's instruction (Gibco, Invitrogen). The cells were cultured in Dulbecco's modified Eagle's medium (DMEM, Substrate Department, University of Copenhagen, Denmark) supplemented with 10% fetal calf serum (Gibco, Invitrogen) and 40 mg·L^{-1} L-proline at 37°C in 5% CO_2.

Electrophysiological recordings of transiently transfected CHO-K1

Whole-cell currents were recorded using an EPC-10 amplifier (HEKA Electronics, Lambrecht, Germany). Data were sampled with Pulse software (HEKA Electronics) and analysed with IGOR software (Wavemetrics, Lake Oswego, OR, USA). The series resistance (R_s) was compensated 80 % and did not exceed 3 MΩ. Electrodes were pulled from borosilicate glass capillaries (Module Ohm, Herlev, Denmark) and had tip resistances between 1.5 and 2.5 MΩ. For the $K_V4.3$/KChIP2/DPP6 experiments shown in Figure 1, recording conditions were identical to those previously used for measuring native I_{to} (Calloe *et al.*, 2009a). Cells were superfused with a HEPES buffer of the following composition (mM): NaCl 126, KCl 5.4, $MgCl_2$ 1.0, $CaCl_2$ 2.0, HEPES 10 and glucose 11, pH adjusted to 7.4 with NaOH. The patch pipette solution had the following composition (mM): K-aspartate 90, KCl 30, glucose 5.5, $MgCl_2$ 1.0, EGTA 5, MgATP 5, HEPES 5, NaCl 10, pH = 7.2 with KOH. In myocytes, I_{to} was recorded in the presence of 300 µM Cd^{2+} which was used to block I_{CaL}. We therefore included 300 µM Cd^{2+} in the present study to allow a more direct comparison.

For CHO-K1 cells expressing $K_V4.3$/KChIP2/DPP6, the membrane capacitance was 14.0 ± 2.2 pF and the mean peak current 7.5 ± 2.0 nA. For the concentration-response experiments on $K_V4.3$/KChIP2 (Figure 3), a standard extracellular NaCl solution consisted of (mM): NaCl 140, KCl 4, $CaCl_2$ 2, $MgCl_2$ 1, HEPES 10, pH = 7.4 adjusted with NaOH was used and the intracellular solution contained (mM): KCl 110, KOH/EDTA 31/10, $CaCl_2$ 5.17, $MgCl_2$ 1.42, HEPES 10, MgATP 4, pH = 7.2 with KOH. The membrane capacitance was 14.9 ± 1.4 pF and the mean peak current in control 7.1 ± 1.4 nA at +20 mV. All experiments were performed at 37 ± 1°C.

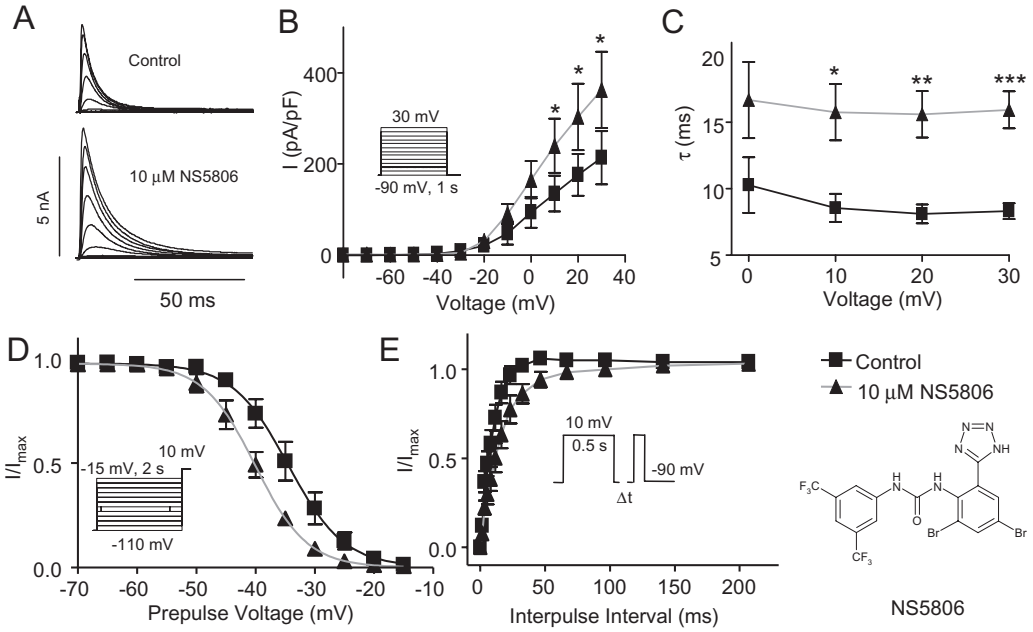

Figure 1

Effect of NS5806 on K_V4.3/KChIP2/DPP6. K_V4.3/KChIP2/DPP6 were transiently expressed in CHO-K1 cells and currents were measured in the absence and in the presence of 10 μM NS5806. (A) Representative recordings of K_V4.3/KChIP2/DPP6 currents elicited by the protocol shown in panel B. (B) Relation between peak current density and voltage, $n = 5$. (C) Mono-exponential functions were fitted to the current decays, and the time constants (τ) are shown as a function of voltage, $n = 7$). (D) Steady-state inactivation of K_V4.3/KChIP2/DPP6 currents. Normalized tail current amplitudes recorded at +10 mV are plotted as a function of the prepulse potential and Boltzmann equations are fitted to the data, $n = 5$. (E) Time-dependent release from inactivation. K_V4.3/KChIP2/DPP6 currents were activated by the depicted two-pulse protocol. Current amplitudes at the second test pulse were normalized to that of the first test pulse and plotted as a function of the inter-pulse interval, and a single exponential equation was fitted to the data, $n = 6$). $^*P < 0.05$, $^{**}P < 0.01$, $^{***}P < 0.001$; significantly different in the absence and presence of NS5806. CHO-K1, Chinese hamster ovary cells; DPP, dipeptidyl-peptidase; KChIP2, K channel interacting protein 2.

Statistics

Mean ± SEM are shown. Statistical significance was evaluated by Student's *t*-test and one way ANOVA with Dunnett's post test as appropriate using GraphPad Prism (GraphPad Software, San Diego, CA, USA).

Results

Effect of NS5806 on K_V4.3/KChIP2/DPP6 channels expressed in CHO-K1 cells

K_V4.3 together with KChIP2 and DPP6 produces a current resembling native I_{to} (Radicke *et al.*, 2005). As an initial basis for comparison, we co-expressed K_V4.3/KChIP2/DPP6 in CHO-K1 cells and recorded currents in solutions identical to those previously used for native I_{to} measurements (Calloe *et al.*, 2009a). As we found with native I_{to}, 10 μM NS5806 induced a 65% increase of K_V4.3/KChIP2/DPP6 peak current amplitudes (Figure 1A and B). The time constant of decay (τ) of I_{to} was significantly slowed as reflected in 80% increase in τ-values over a range of voltages (Figure 1C). Steady-state gating parameters were evaluated using a pre-pulse-test pulse voltage clamp protocol. The peak current following a 2 s prepulse was normalized to the maximum current and plotted as a function of prepulse voltage to obtain the availability of channels. A Boltzmann curve was fitted to the data and the mid-inactivation voltage ($V_{1/2}$) was determined. NS5806 induced a significant left-shift in mid-inactivation from –34.5 ± 0.6 mV to –40 ± 0.4 mV (Figure 1D), indicating a tendency for a larger fraction of channels being in the inactivated state in presence of NS5806, as observed for native I_{to} (Calloe *et al.*, 2009b).

Time-dependent recovery from inactivation of K_V4.3/KChIP2/DPP6 was evaluated by a two-pulse protocol with increasing interpulse intervals. The fraction of recovered current was plotted as a function of interpulse interval and an exponential equation fitted to the data. NS5806 significantly slowed recovery of K_V4.3/KChIP2/DPP6 current, with time constants of 9.3 ± 0.6 ms prior to NS5806 application versus 16.4 ± 1.2 ms after application of 10 μM NS5806. These results were opposite to the effect of NS5806 on I_{to} recorded in isolated canine ventricular cardiomyocytes where recovery of I_{to} was faster in the presence of NS5806.

Concentration-dependence of the effect of NS5806 on K_V4.3/KChIP2/DDP6 channels

To characterize NS5806, we initially tested the concentration-dependent effect of NS5806 on peak current amplitude and time course of current inactivation of Kv4.3/KChIP2 expressed in CHO-K1 cells. NS5806 increased peak-current amplitudes concentration-dependently with an EC_{50} value of 5.3 ± 1.5 μM and the time course of inactivation (τ) was slowed with an EC_{50} value of 25.4 ± 1.1 μM (Figure 2).

To further test the effect of NS5806 on different ion channels and multiple combinations of ion channel subunits we used *Xenopus laevis* oocytes as cRNA encoding ion channel subunits can be injected directly into the oocytes, ensuring better control over subunit ratios than the transfection procedure of mammalian cell lines. In this series of experiments, K_V4.3 was expressed in *Xenopus laevis* oocytes in absence or presence of KChIP2 and DPP6 and currents measured in presence of 0 to 30 μM NS5806 (Figure 3A). Interestingly, the K_V4.3 peak current amplitude was reduced by NS5806, whereas NS5806 caused a minor increase in K_V4.3/KChIP2 and K_V4.3/KChIP2/DPP6 peak current amplitude as well as a pronounced slowing of current decay. In contrast to K_V4.3/KChIP2/DPP6 expressed in CHO-K1 cells and native I_{to} (Calloe *et al.*, 2009a,b) the effect of NS5806 on K_V4.3/KChIP2 peak current amplitude in *Xenopus laevis* oocytes was minor. The slowing of current decay was concentration-dependent and qualitatively similar with and without DPP6. For K_V4.3 expressed alone, there was no effect on the decay even at higher concentrations of NS5806 (Figure 3B). A sigmoidal concentration-response curve was fitted to K_V4.3/KChIP2 current decay and an EC_{50} 18.8 ± 2.0 μM was calculated. For all subunit combinations, the effect of NS5806 was rapid and fully reversible, as illustrated by the representative K_V4.3/KChIP2 time-course experiment (Figure 3C).

Effect of NS5806 on K_V4 family channels in presence or absence of KChIP2

To investigate if NS5806 affected other members of the K_V4 family and whether this effect also depended on KChIP2, all K_V4 family α-subunits were expressed with and without KChIP2 in oocytes. Currents were activated by depolarizing voltage steps from a holding potential of –100 mV. For K_V4.2 and K_V4.3, NS5806 had no effect on current amplitude, in contrast to the results presented for K_V4.3 in Figure 3, where a holding potential of –80 mV was used. For all K_V4 channels, co-expression with KChIP2 resulted in higher current amplitudes and a significantly slower current decay (Figure 4 and

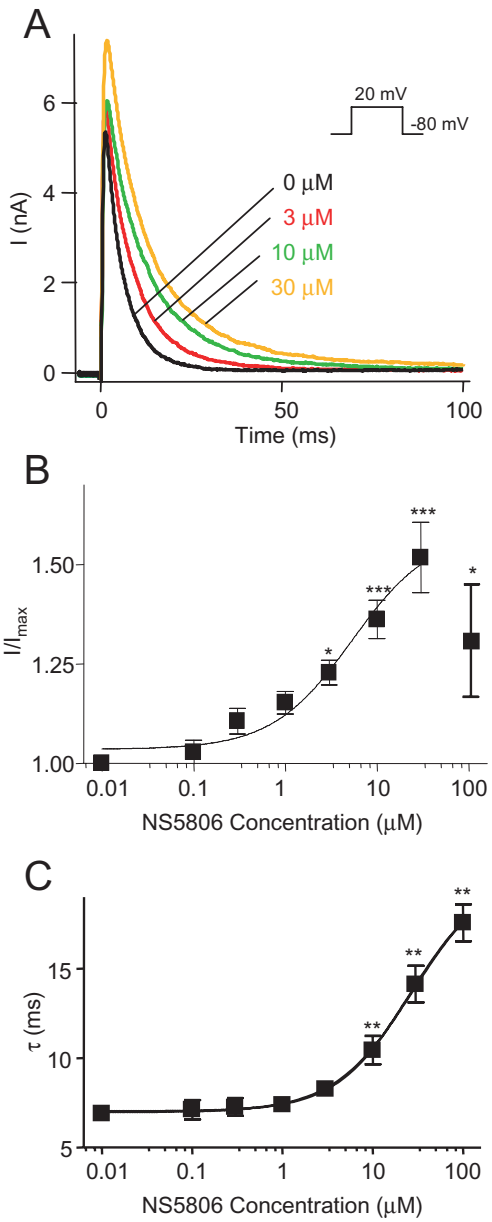

Figure 2

Concentration dependent effect of NS5806 on K_V4.3/KChIP2 in CHO-K1 cells. K_V4.3 and KChIP2 were transiently expressed in CHO-K1 cells and measured in presence of 0 to 100 μM NS5806 as indicated in the figure. (A) Representative current recordings at different NS5806 concentrations. (B) Peak current amplitudes normalized to current amplitudes in absence of drug and plotted as function of NS5806 concentration. A sigmoidal dose-response curve was fitted to the data in the range from 0–30 μM and an EC_{50} of 5.3 ± 1.5 μM with and a Hill slope of 1.1 ± 0.05 and minimum and maximum values of 1.04 ± 0.02 and 1.6 ± 0.06 respectively. (C) Effect of different NS5806 concentrations on Kv4.3/KChIP2 decay. The time-constants, τ, were plotted as function of NS5806 concentration and revealed an EC_{50} of 25.4 ± 1.1 μM. The Hill slope was 1.08 ± 0.06 with minimum and maximum values of 7.0 ± 0.1 ms and 20.0 ± 0.5 ms respectively (n = 7–12). *P < 0.05, **P < 0.01, ***P < 0.001; significantly different in the absence and presence of NS5806. CHO-K1, Chinese hamster ovary cells; KChIP2, K channel interacting protein 2.

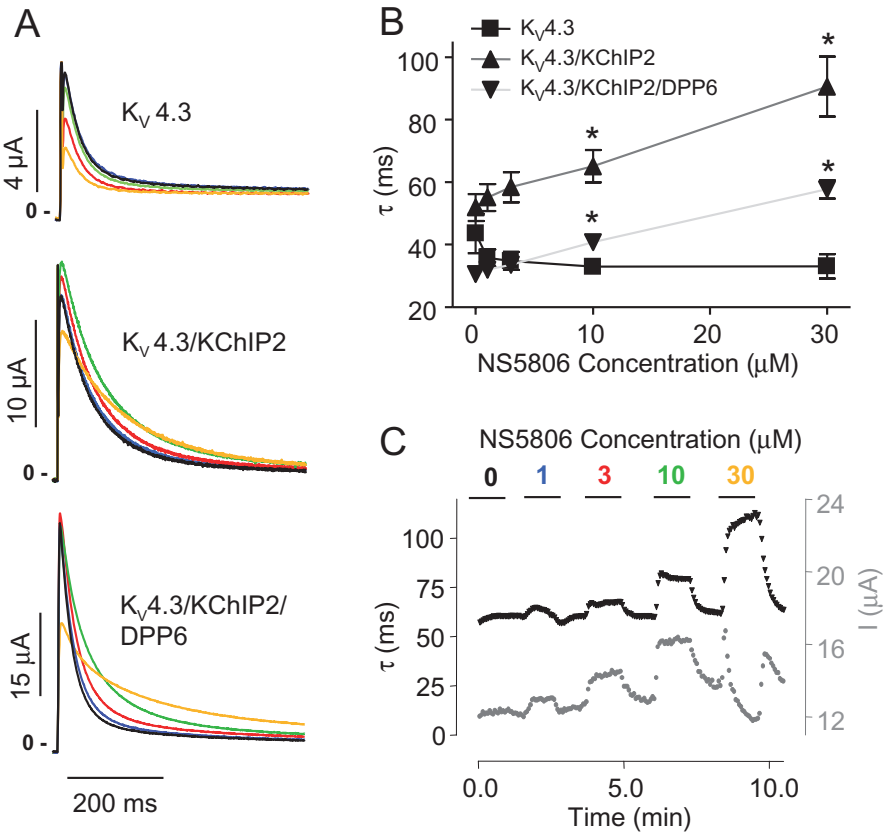

Figure 3

Concentration dependent effect of NS5806 on $K_V4.3$, KChIP2 and DPP6 in *Xenopus laevis* oocytes. $K_V4.3$, KChIP2 and/or DPP6 were expressed in *Xenopus laevis* oocytes. Currents were repeatedly activated from –80 mV by steps to +40 mV. (A) Representative recordings of $K_V4.3$, $K_V4.3$/KChIP2 and $K_V4.3$/KChIP2/DPP6 currents in presence of 0 (black), 1 (blue), 3 (red) 10 (green) or 30 (orange) µM NS5806. (B) Single exponential functions were fitted to the first 150 ms of $K_V4.3$, $K_V4.3$/KChIP2 and $K_V4.3$/KChIP2/DDP6 current decays and the time constants (τ) are plotted as a function of NS5806 concentration (n = 6–8). *P < 0.05, significantly different in the absence and presence of NS5806. (C) $K_V4.3$/KChIP2 time-course experiment. The black trace shows the effect of increasing concentrations of NS5806 on $K_V4.3$/KChIP2 peak current decay (τ; lefthand Y axis) and the grey trace shows the effect on the peak current amplitude (I, righthand Y axis), representative of n = 6. DPP, dipeptidyl-peptidase; KChIP2, K channel interacting protein 2.

Table 1). NS5806 had no effect on current decay of $K_V4.2$ and $K_V4.3$, whereas it markedly slowed the decay in presence of KChIP2 (Figure 4B and C). For $K_V4.1$, NS5806 slowed current decay both in presence and absence of KChIP2 (Figure 4A).

Slowing of K_V4/KChIP2 current decay resulted in an increase in total charge movement in presence of the drug, as assessed by the area under the current traces (Table 1 and Supplementary Figures S1 and 2). To evaluate steady-state mid-inactivation ($V_{1/2}$) of K_V4 and K_V4/KChIP2 channels, peak tail-currents following a 2 s prepulse were normalized to the maximal current and a Boltzmann equation was fitted to the data. For all channel complexes, 10 µM NS5806 caused a prominent left-shift in $V_{1/2}$ (Tables 1 and 2 and Supplementary Figures S1 and S2), and as illustrated for $K_V4.3$ and $K_V4.3$/KChIP2 in Figure 5A and B. This negative shift in $V_{1/2}$ explains the disparate effects of NS5806 on $K_V4.3$ peak currents (Figures 3B and 4C, Tables 1 and 2) when using –80 mV or –100 mV as holding potential. As –80 mV is close to physiological resting membrane potentials, we used –80 mV as holding in the following studies. Recovery from inactivation for K_V4 and K_V4/KChIP2 channels expressed in *Xenopus laevis* oocytes was addressed by a standard two-pulse protocol and was found to be slowed by 10 µM NS5806 for all K_V4 and K_V4/KChIP2 channels (Table 1, Figure 5C and D and Supplementary Figures S1 and 2).

The negative shift in mid-inactivation $V_{1/2}$ suggests that NS5806 increases closed-state inactivation. Closed-state inactivation of $K_V4.3$ and for $K_V4.3$/KChIP2 expressed in *Xenopus laevis* oocytes was addressed by a modified double-pulse protocol (Bahring *et al.*, 2001). After the first test-pulse, inactivation was completely released by a hyperpolarizing step to –100 mV followed by a step to a voltage

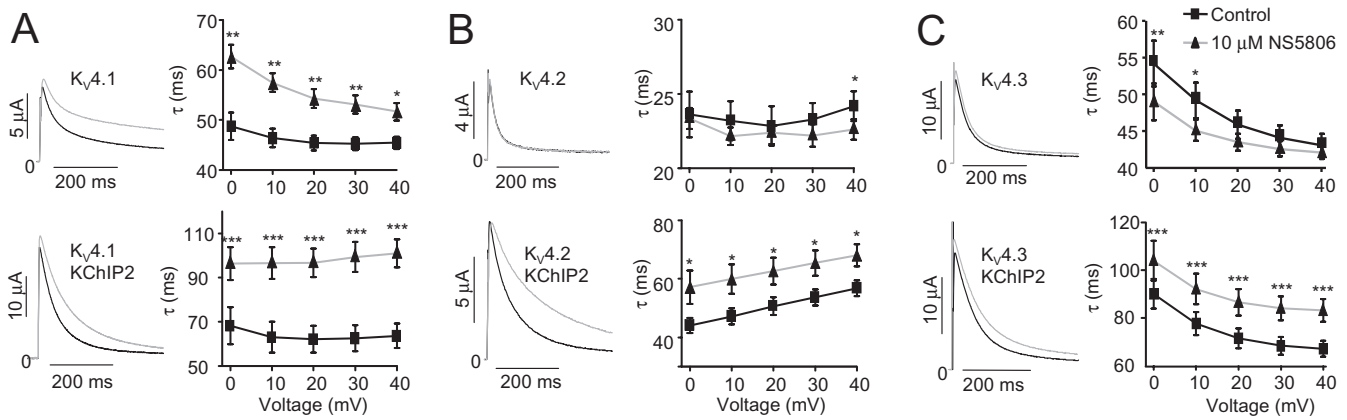

Figure 4

Effect of NS5806 on K_V4 channels in presence or absence of KChIP2. K_V4 channels were expressed with and without KChIP2 in *Xenopus laevis* oocytes and currents were elicited from a holding potential of −100 mV by a step to +40 mV in absence and presence of 10 μM NS5806. The first 150 ms of current decay was fitted to a mono-exponential function, and the time constants (τ) are shown as a function of voltage. (A) Representative K_V4.1 (n = 5) and K_V4.1/KChIP2 currents (n = 6) and τ-values as a function of voltage before and after application of drug. (B) Representative K_V4.2 (n = 6) and K_V4.2/KChIP2 (n = 10) currents and τ-values as a function of voltage. (C) Representative K_V4.3 (n = 8) and K_V4.3/KChIP2 (n = 8) currents and τ-values as a function of voltage. *P < 0.05, **P < 0.01, ***P < 0.001; significantly different in the absence and presence of NS5806. KChIP2, K channel interacting protein 2.

below the activation threshold (−50 mV) allowing for onset of closed-state inactivation for increasing time intervals before application of a second test pulse. The current amplitude at the second pulse was plotted as a function of interpulse interval and a mono-exponential decay function was fitted to the data (Figure 6). Both in the presence and absence of KChIP2, NS5806 significantly accelerated the onset of closed-state inactivation. For K_V4.3, the time constant (τ) of closed-state inactivation was 701 ± 203 ms before and 164 ± 29 ms after application of 10 μM NS5806 and for K_V4.3/KChIP2, τ = 838 ± 338 ms before, and 310 ± 80 ms after application of NS5806.

Effect of NS5806 on K_V4.3 expressed with various ancillary subunits

For K_V4.3/KChIP2 currents in CHO-K1 cells and in *Xenopus laevis* oocytes, the time dependent recovery from inactivation was slowed by NS5806 (Figure 1E and Figure 5C and D); however, for native I_{to} the recovery was accelerated by 10 μM NS5806 (Calloe *et al.*, 2009a). As ancillary subunits can dramatically change the effect of exogenous compounds (Bett and Rasmusson, 2008), we wondered if the difference between I_{to} and K_V4.3/KChIP2 currents could be due to presence of additional ancillary subunits in the native I_{to} channel complex. In the next series of experiments we evaluated the effect of 10 μM NS5806 on K_V4.3 expressed with and without KChIP2 and the putative I_{to} ancillary subunits DPP6, DPP10, KCNE2 and KCNE3 and the results are summarized in Table 2.

Comparing the control recordings revealed that DPP6 and DPP10 increased K_V4.3 and K_V4.3/KChIP2 currents and accelerated current decay. KCNE2 inhibited K_V4.3 and K_V4.3/KChIP2 current amplitude as also reported by Radicke *et al.* (2006). In agreement with our previous findings (Lundby and Olesen, 2006; Delpón *et al.*, 2008), KCNE3 reduced both K_V4.3 and K_V4.3/KChIP2 currents. Interestingly, it appeared that this inhibition of current could be abolished by co-expressing K_V4.3/KCNE3 with DPP6 (Table 2). Addressing the effect of NS5806 on the different subunit combinations, we found NS5806 exclusively caused a slowing of the current decay (τ) in channel complexes encompassing KChIP2. Thus, KChIP2 expression appears to be central for the effect of NS5806 on current decay and suggests that KChIP2 is part of the native I_{to} channel. Co-expression of K_V4.3/KChIP2 or K_V4.3/KChIP2/DPP6 with KCNE2 resulted in a marked slowing in recovery from inactivation following application of NS5806. These results are opposite to the effects seen in canine I_{to}. NS5806 accelerated K_V4.3/KChIP2/DPP10 current decay suggesting that DPP10 is an unlikely candidate for the native I_{to} channel. For all subunit combinations tested, application of NS5806 slowed recovery from inactivation, in sharp contrast to the acceleration of recovery observed in native I_{to} channels.

Effect of NS5806 on other cardiac potassium channels

The effect of 10 μM NS5806 was further tested on α-subunits mediating other important repolarizing

Table 1

Effect of 10 μM NS5806 on K_v4 channels in absence or presence of KChIP2

	$K_v4.1$	$K_v4.1$/KChIP2	$K_v4.2$	$K_v4.2$/KChIP2	$K_v4.3$	$K_v4.3$/KChIP2
Peak current (μA) control	12.2 ± 1.1	23.6 ± 1.3	1.9 ± 0.3	6.6 ± 1.4	13.8 ± 1.2	23.2 ± 1.2
10 μM NS5806	12.6 ± 1.0 (5)	27.0 ± 1.3 (6)***	2.0 ± 0.3 (6)	7.5 ± 1.3 (10)*	15.3 ± 1.4 (11)	26.9 ± 1.3 (9)***
Decay τ (ms) control	45.4 ± 1.2	63.6 ± 5.5	24.2 ± 1.1 (6)	56.8 ± 2.7	44.2 ± 1.9	67.2 ± 3.4
10 μM NS5806	51.7 ± 1.8 (5)*	101 ± 6.2 (8)***	22.6 ± 0.7 (6)*	68.1 ± 3.8 (10)*	43.5 ± 1.5 (11)	83.2 ± 4.7 (9)***
Area (μA·ms^{-1}) control	814 ± 70	2260 ± 181	66 ± 9.8	378 ± 74	762 ± 63.9	1450 ± 103
10 μM NS5806	1250 ± 109 (5)**	3150 ± 166 (8)***	67 ± 10 (6)	533 ± 101 (10)**	825 ± 84 (11)	1890 ± 142 (8)**
$V_{1/2}$ (mV) control	–60.8 ± 0.85	–44.7 ± 0.7	–65.2 ± 1.1	–57.3 ± 0.9	–55.4 ± 0.5	–48.6 ± 0.4
10 μM NS5806	–75 ± 1.8 (5)***	–59.5 ± 0.5 (8)***	–75.7 ± 1.9 (6)***	–67.1 ± 1.3 (10)***	–66.0 ± 1.0 (10)***	–54.0 ± 1.1 (8)**
Recovery τ (ms) control	80.8 ± 3.5	8.0 ± 2.8	110 ± 29	12.6 ± 3.0	95.8 ± 2	15.9 ± 0.5
10 μM NS5806	205 ± 31 (5)***	37.1 ± 10 (8)***	202 ± 54 (6)**	26.4 ± 1.8 (10)***	221 ± 8 (8)***	23.7 ± 0.48 (8)***

K_v4 channels expressed with and without KChIP2 (1:1 molar ratio) in *Xenopus laevis* oocytes. Currents were activated from a holding potential of –100 mV by a +40 mV step before and during application of 10 μM NS5806 and peak current amplitudes, time constants (τ) of current decay and total charge movement for the first 150 ms after complete activation was measured. Steady-state mid-inactivation ($V_{1/2}$) was evaluated from a holding potential of –100 mV by a series of 2 s prepulses from –100 to +40 mV followed by a +40 mV step. Boltzmann equations were fitted to normalized tail current amplitudes plotted as a function of the prepulse potential. Time constants (τ) for recovery from inactivation was determined by a two-pulse protocol; from a holding potential of –80 mV currents were activated by two test potentials to +40 mV with increasing interpulse time. The peak current at the second pulse was normalized to the first pulse and single exponential functions were fitted to the data points. The different K_v4 α-subunits were recorded on different days; however, the experiments in absence and presence of KChIP2 were performed in parallel and thus current amplitude and biophysical characteristics can be directly compared.
*$P < 0.05$, **$P < 0.01$, ***$P < 0.001$; significantly different in the absence and presence of NS5806.
KChIP2, K channel interacting protein 2.

Table 2

Effect of 10 μM NS5806 on K_V4.3 co-expressed with different subunits

Kv4.3+	–	DPP6	KCNE2	KCNE3	DPP6/KCNE3	KChIP2/DPP10
Peak current (μA) control	14.4 ± 2.0	20.4 ± 1.4	12.1 ± 1.9	1.8 ± 0.18	37.8 ± 6.8	14 ± 1.4
10 μM NS5806	6.6 ± 1.3 (8)**	11.0 ± 1.7 (9)***	7.5 ± 1.5 (6)**	1.3 ± 0.28 (8)*	23.6 ± 5.8 (8)**	10.4 ± 1.1 (5)**
Decay τ (ms) control	42.4 ± 2.1	37.7 ± 2.7	66.4 ± 13.8	55.1 ± 4.7	31.0 ± 1.0	17.6 ± 0.8
10 μM NS5806	45.6 ± 3.6 (8)	28.8 ± 0.73 (9)*	52.4 ± 7–3 (6)	48.1 ± 1.9 (4)	28.2 ± 7.7 (8)*	11.9 ± 0.5 (5)***
Area (μA·ms^{-1}) control	783 ± 102	939 ± 120	959 ± 251	176 ± 45	1415 ± 311	409 ± 23
10 μM NS5806	367 ± 59 (8)***	501 ± 88 (9)***	408 ± 88 (6)**	169 ± 49 (4)	877 ± 20 (9)**	188 ± 194 (5)***
$V_{1/2}$ (mV) control	−56.8 ± 1.3	−75.2 ± 0.14	−59.6 ± 0.9	−60.1 ± 0.57	−78.6 + 0.3	−72.8 ± 0.5
10 μM NS5806	−80.7 ± 2.7 (8)***	−82.2 ± 0.14 (8)***	−79.9 ± 1.1 (6)***	−78.4 ± 1.1 (8)***	−81.7 ± 0.2 (9)***	−80.6 ± 0.4 (5)***
Recovery τ (ms) control	480 ± 71	159 ± 3.8	235 ± 13.4	543 ± 24	176 ± 1.9	93.9 ± 2.1
10 μM NS5806	1459 ± 10 (8)***	239 ± 2.2 (5)***	492 ± 94.6 (6)***	1237 ± 123 (8)***	252 ± 2.4 (10)***	86.6 ± 6.3 (5)
Kv4.3+	**KChIP2**	**KChIP2/DPP6**	**KChIP2/KCNE2**	**KChIP2/KCNE3**	**KChIP2/DPP6/KCNE3**	**KChIP2/DPP6/KCNE2**
Peak current (μA) control	33.9 ± 2.9	33.1 ± 8.5	13.9 ± 1.47	1.8 ± 0.36 (5)	24.7 ± 3.9	33.9 ± 1.3
10 μM NS5806	35.9 ± 3.1 (7)**	33.0 ± 9.5 (9)	10.7 ± 1.09 (9)***	1.5 ± 0.36 (5)*	25.3 ± 4.0 (9)	25.9 ± 1.4 (5)**
Decay τ (ms) control	65.5 ± 6.3	33.6 ± 1.6	72.0 ± 6.5	187 ± 38	37.0 ± 2.1	44.3 ± 3.0
10 μM NS5806	90.0 ± 14.9 (7)***	45.3 ± 1.0 (10)***	78.0 ± 6.2 (9)*	199 ± 100(5)	42.1 ± 1.3 (9)*	44.9 ± 1.9 (5)
Area (μA·ms^{-1}) control	2011 ± 219	1111 ± 304	1140 ± 98	195 ± 86	1190 ± 224	1804 ± 310
10 μM NS5806	2702 ± 316 (7)***	1752 ± 498 (10)*	822 ± 101 (9)*	153 ± 84 (5)	1622 ± 325 (9)**	1616 ± 98 (5)*
$V_{1/2}$ (mV) control	−50.2 ± 0.7	−63 ± 0.4	−52.44 ± 1.3	−60.4 ± 1.3 (5)	−71.4 ± 0.6	−70.2 ± 0.4
10 μM NS5806	−58.9 ± 0.7 (7)***	−69 ± 0.3 (4)***	−71.9 ± 2.2 (9)***	−79.9 ± 1.5 (5)***	−77.8 ± 0.43 (9)***	−78.2 ± 0.2 (5)***
Recovery τ (ms) control	76.6 ± 2	42.6 ± 1.8	189.1 ± 5.5	522 ± 56 (5)	62.6 ± 1.6	68.6 ± 1.1
10 μM NS5806	274 ± 8.0 (7)***	66.8 ± 3.1 (8)***	547 ± 151 (9)***	1304 ± 134 (5)***	99.1 ± 1.6 (5)***	106 ± 4.5 (5)***

K_V4.3 channels expressed with different accessory subunits in *Xenopus laevis* oocytes. Currents were activated from a holding potential of −80 mV by a +40 mV step before and during application of 10 μM NS5806 and peak current amplitudes, time constants (τ) of current decay and total charge movement for the first 150 ms after complete activation was measured. Steady-state mid-inactivation ($V_{1/2}$) was evaluated from a holding potential of −100 mV by a series of 2 s prepulses from −100 to +40 mV followed by a +40 mV step. Boltzmann equations were fitted to normalized tail current amplitudes plotted as a function of the prepulse potential. Time constants (τ) for recovery from inactivation was determined by a two-pulse protocol; from a holding potential of −80 mV currents were activated by two test potentials to +40 mV with increasing interpulse time. The peak current at the second pulse was normalized to the first pulse and single exponential functions were fit to the data points. The different K_V4.3 β-subunit combinations were recorded on different days; however, the experiments in absence and presence of KChIP2 were in all cases performed in parallel and thus current amplitude and biophysical characteristics can be directly compared.
*P < 0.05, **P < 0.01, ***P < 0.001; significantly different in the absence and presence of NS5806.
DPP, dipeptidyl-peptidase.

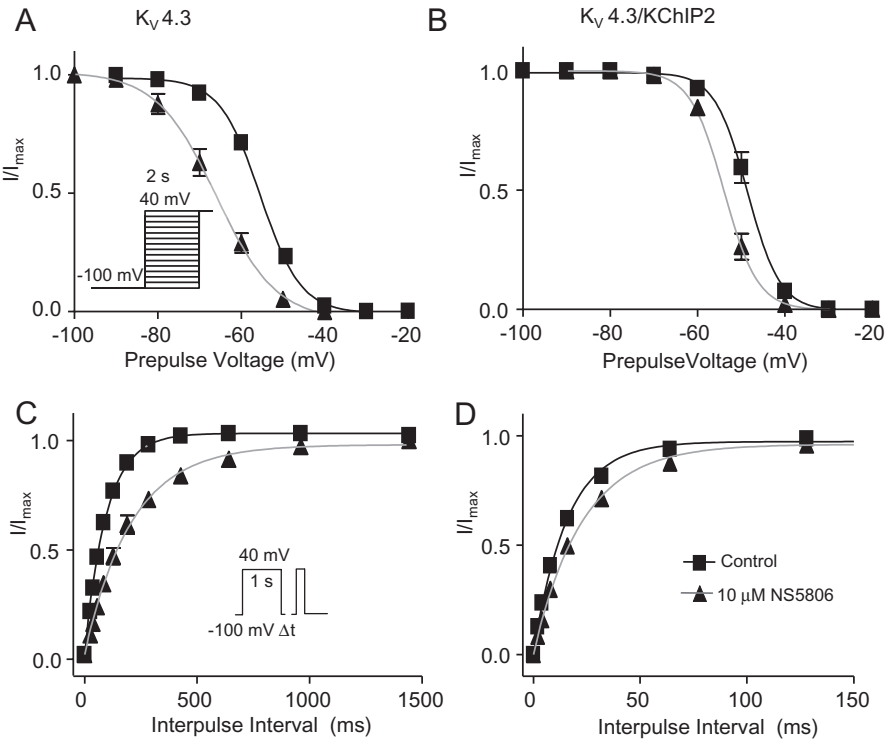

Figure 5

Effect of NS5806 on steady-state inactivation and time dependent recovery of K_V4.3 and K_V4.3/KChIP2 channels. K_V4.3 and K_V4.3/KChIP2 were expressed in *Xenopus laevis* oocytes. Steady-state inactivation was evaluated before (squares) and after application of 10 μM NS5806 (triangles). Normalized tail current amplitudes plotted as a function of the prepulse potential for currents elicited by the depicted voltage-clamp protocol and Boltzmann equations were fitted to the data. (A) Steady-state inactivation of K_V4.3, $n = 10$. (B) Steady-state inactivation of K_V4.3/KChIP2, $n = 9$. Time-dependent recovery from inactivation at –100 mV was addressed by a two-pulse protocol with an increasing inter-pulse interval as shown. The peak current at the second pulse was normalized to the current at the first pulse and a single exponential equation was fitted to the data. (C) Time-dependent recovery of K_V4.3, $n = 8$. (D) Time-dependent recovery of K_V4.3/KChIP2, $n = 8$. KChIP2, K channel interacting protein 2.

cardiac potassium currents. K_V1.4 and K_V1.5 were expressed in *Xenopus laevis* oocytes in the presence or absence of KChIP2. For K_V1.4, 10 μM NS5806 inhibited more than 80% of the current (Figure 7A). The effect on the related K_V1.5 channel was smaller and mainly on the sustained current (Figure 7C). For both K_V1.4 and K_V1.5, co-expression with KChIP2 did not affect basal currents or the response to NS5806 (Figure 7B and D). There was no effect of NS5806 on currents generated by K_V11.1, K_V7.1 and K_{ir}2.1-3 channels (Supplementary Figures S3–5).

Are other α-subunits contributing to canine ventricular I_{to}?

I_{to} measured in isolated cells from canine left ventricular epi- and midmyocardium recovers from inactivation with a bi-exponential time-course. Besides increasing currents and accelerating the recovery, the time-course of the recovery is changed from bi-exponential to mono-exponential in the presence of NS5806 (Calloe *et al.*, 2009b).This might be explained by NS5806 enhancing a fast recovering current and inhibiting a slower recovering current. Thus, to test how NS5806 would affect a current generated by a mixture of the slowly recovering K_V1.4 (Supplementary Figure S6A) and the fast recovering K_V4.3/KChIP2/DPP6 channels, we co-expressed the channel constructs in *Xenopus laevis* oocytes in a 1:1 current ratio. Peak-current amplitude was unaffected by 10 μM NS5806 (Figure 8A), current decay was slowed (Figure 8B) and there was a significant left shift in steady-state mid-nactivation $V_{1/2}$, from –53.0 ± 0.8 mV to –67.7 ± 1.3 mV (Figure 8C). Recovery from inactivation was addressed as previously described and the fraction of recovered current was plotted as a function of interpulse time and a bi-exponential function was fitted to the data (Figure 8D and E). For control, the recovery showed a slow and a fast phase, $\tau_1 = 20.1 \pm 2.6$ ms (relative weight of the pre-exponential factor, $A_1 = 0.30 \pm 0.04$) and $\tau_2 = 1155 \pm 448$ ms (relative weight of the pre-exponential factor, $A_2 = 0.70 \pm 0.03$) respectively. In the presence of NS5806 the reactivation time course was markedly faster with $\tau_1 = 26.0 \pm 1.9$ ms ($A_1 = 0.95 \pm 0.04$) and $\tau_2 = 411 \pm 242$ ms ($A_2 = 0.05 \pm 0.03$). In the presence of

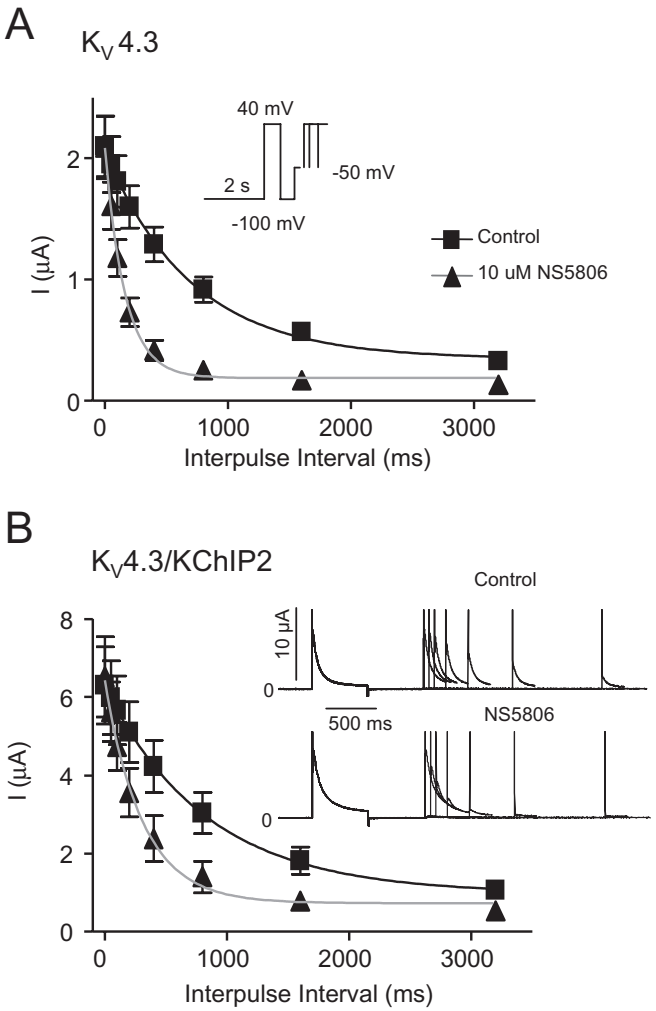

Figure 6

Effect of NS5806 on closed-state inactivation of K_V4.3 and K_V4.3/KChIP2 channels. K_V4.3 and K_V4.3/KChIP2 were expressed in *Xenopus laevis* oocytes. Closed-state inactivation was evaluated before and after application of 10 μM NS5806. Currents were activated from a holding of −100 mV by a brief +40 mV step. Inactivation was completely released by a −100 mV step and followed by a step at a voltage below the activation threshold (−50 mV) at increasing time-intervals before currents were activated by a second +40 mV step. Current amplitude at the second pulse is plotted as a function of pulse interval time for K_V4.3, n = 9 (A) and for K_V4.3/KChIP2, n = 5 (B). Representative K_V4.3/KChIP2 currents are shown in panel B. KChIP2, K channel interacting protein 2.

NS5806, the pre-exponential factor of the slow component was small and the reactivation could be fitted with a mono-exponential equations with τ = 30.8 ± 1.2 ms. Thus, the recovery of the K_V4.3/KChIP2/DPP6/K_V1.4 current from inactivation was qualitatively similar to that of native I_{to} in the absence and presence of NS5806. Similar results were found for K_V4.3/KChIP2/K_V1.4 (Supplementary Figure S6B).

Discussion and conclusion

Effects of NS5806 on K_V4.3 channel gating

NS5806 increased peak current amplitude of Kv4.3/KChIP2 expressed in CHO-K cells with an EC_{50} of 5.3 ± 1.5 μM and slowed the time course of current inactivation (τ) with an EC_{50} of 25.4 ± 1.1 μM. For Kv4.3/KChIP2 expressed in *Xenopus laevis* oocytes, the effect of the compound was mainly on current decay. Ancillary subunits can modify channel gating and may induce conformational changes that can affect access or affinity for exogenous compounds (Bett and Rasmusson, 2008) and the effect of NS5806 on current decay appeared to be linked to KChIP2. KChIP2 is a cytosolic protein that interacts with the intracellular N-termini of K_V4 subunits (Callsen *et al.*, 2005); however, NS5806 also affected K_V4 channels in the absence of KChIP2, as evident from the shift in mid-inactivation, suggesting the binding site is on the α-subunit.

The negative shift in the mid-inactivation observed for all subunit combinations tested indicates that NS5806 increased closed-state inactivation, which was confirmed in a set of experiments addressing the onset of closed-state inactivation for K_V4.3 in the presence and absence of KChIP2. For K_V4.3 and K_V4.3/KChIP2, NS5806 increased the fraction of channels that entered closed-state inactivation.

Recovery from closed-state inactivation has been suggested to be the limiting factor for K_V4 channel recovery (Bahring *et al.*, 2001; Amadi *et al.*, 2007). In agreement, we show that the time-dependent recovery of K_V4 channels was slowed in the presence of NS5806. The faster onset of closed state inactivation and slower recovery from inactivation results in a larger fraction of K_V4 channels being in an inactivated state, mainly in the absence of KChIP2. Thus, NS5806 modified Kv4.3/KChIP2 gating in several ways that inhibit current. This dual mode of activation and inhibition may explain why 100 μM NS5806 increased Kv4.3/KChIP2 peak-currents less than 30 μM did in CHO-K1 cells. However, it should be emphasized that in canine ventricular cardiomyocytes and in CHO-K1 cells, the prominent effect of 10 μM NS5806 was to increase the size of current. The mechanisms behind the observed increase in peak current are unknown, for K_V4.3/KChIP2 channels it could be due to slowed inactivation; however, this is an unlikely mechanism for the increase in Kv4.3 currents in the absence of KChIP2 as current decay is unaffected in the absence of KChIP2 and the exact mechanism of drug binding and how drug binding is transmitted to a response is not known.

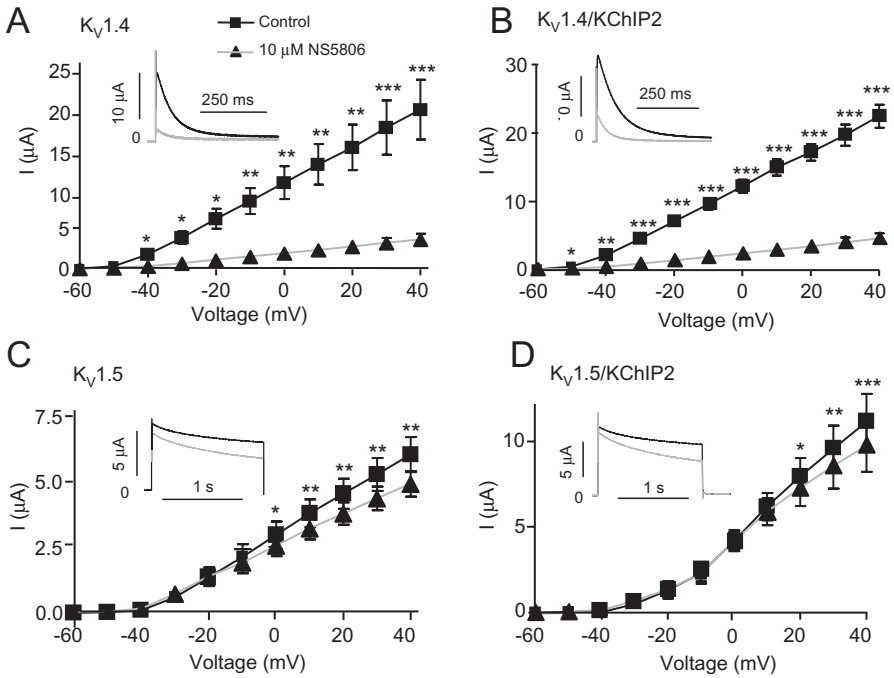

Figure 7

Effect of NS5806 on K_V1.4 and K_V1.5 channels in presence or absence of KChIP2. K_V1.4 and K_V1.5 were expressed with and without KChIP2 in *Xenopus laevis* oocytes. Currents were activated from a holding potential of –80 mV to voltage steps from –100 mV to +40 mV before (squares) and after application of 10 µM NS5806 (triangles). Peak current amplitudes as function of voltage and representative current traces are shown for K_V1.4, $n = 5$ (A), K_V1.4/KChIP2, $n = 5$ (B), Kv1.5, $n = 9$ (C) and K_V1.5/KChIP2, $n = 10$ (D). $^*P < 0.05$, $^{**}P < 0.01$, $^{***}P < 0.001$; significantly different in the absence and presence of NS5806. KChIP2, K channel interacting protein 2.

Differential effect of NS5806 on K_V4.3 and K_V4.3/KChIP2 channels – can NS5806 be used to discriminate the molecular composition of native I_{to}?

We have previously characterized the effect of NS5806 on native canine I_{to} in isolated cardiomyocytes. For mid- and epicardial cells, NS5806 increased I_{to} peak current, slowed current decay, caused a negative shift in the steady-state mid-inactivation and accelerated the time dependent recovery from inactivation. As an initial basis for comparison, K_V4.3 was co-expressed with KChIP2 in CHO-K1 cells and *Xenopus laevis* oocytes (Calloe *et al.*, 2009b). In neither expression system did the measured current recapitulate native I_{to} fully, in terms of the response to NS5806. Interestingly K_V4.3 current decay was slowed when KChIP2 was co-expressed, but unaffected in the absence of KChIP2.

As K_V4.3 co-expressed with KChIP2 and DPP6 in heterologous systems has been demonstrated to result in currents with kinetics similar to those of I_{to} in human ventricular cardiomyocytes (Radicke *et al.*, 2005), we first co-expressed K_V4.3 with KChIP2 and DPP6 in CHO-K1 cells in the present study. Currents were measured using similar solutions as for native I_{to}. Similar to native I_{to}, peak current density was increased by NS5806, the current decay slowed and mid-inactivation $V_{1/2}$ shifted to more negative voltages. However, in contrast to the effect on native I_{to}, the time dependent recovery from inactivation was markedly slowed for K_V4.3/KChIP2/DPP6 currents in the presence of NS5806.

We therefore tested the effect of NS5806 on K_V4.3 expressed with KChIP2 and other ancillary subunits in *Xenopus laevis* oocytes. In agreement with our previous observations, current decay was slowed by NS5806 only for K_V4.3 co-expressed with KChIP2, independently on the presence of other ancillary subunits. This implies that NS5806 potentially can be used to investigate the molecular composition of native I_{to} channels. Furthermore, for K_V4.3 channels expressed in the absence of KChIP2, NS5806 may inhibit currents at physiological resting membrane potentials due to the negative shift in the steady-state mid-inactivation (Figure 5 and Table 2).

NS5806 induced a marked increase in peak I_{to} and slowed I_{to} decay in canine mid- and epicardial I_{to} (Calloe *et al.*, 2009a,b) suggesting that KChIP2 is an integral part of the I_{to} channel in canine ventricle. However, none of the tested ancillary subunit

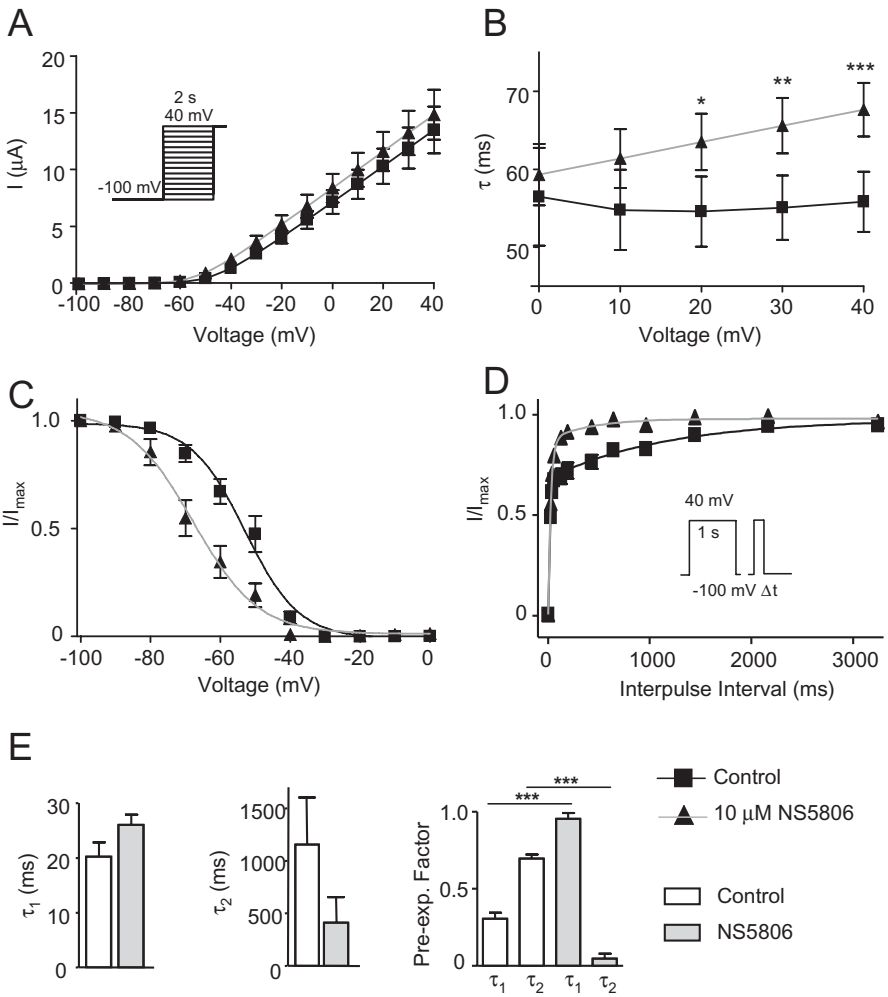

Figure 8

Effect of NS5806 on K_V4.3/KChIP2/DPP6 co-expressed with K_V1.4 channels. K_V4.3/KChIP2/DPP6 and K_V1.4 were co-expressed in *Xenopus laevis* oocytes in a 1:1 current ratio. Currents were elicited using the depicted voltage protocol and measured in the absence and in the presence of 10 μM NS5806. (A) Relation between peak current density and voltage, $n = 8$. (B) Single exponential equations were fitted to the current decays, and the time constants (τ) are shown as a function of voltage, $n = 8$. (C) Steady-state inactivation of K_V4.3/KChIP2/DPP6/K_V1.4 currents. Normalized tail current amplitudes are plotted as a function of the prepulse potential and Boltzmann equations are fitted to the data, $n = 8$. (D) Time-dependent recovery from inactivation. K_V4.3/KChIP2/DPP6/K_V1.4 currents were activated by a two-pulse protocol. Current amplitudes at the second test pulse were normalized to that of the first test pulse and plotted as a function of the inter-pulse interval and double-exponential equations were fitted to the data, $n = 7$. (E) Bar graph showing the time-constants of K_V4.3/KChIP2/DPP6/K_V1.4 recovery from inactivation, τ_1 and τ_2 as well as pre-exponential factors. $^*P < 0.05$, $^{**}P < 0.01$, $^{***}P < 0.001$; significantly different in the absence and presence of NS5806. DPP, dipeptidyl-peptidase; KChIP2, K channel interacting protein 2.

combinations completely reconstituted native canine mid- and epicardial I_{to} with regard to the effect of NS5806. For native I_{to}, the recovery from inactivation was accelerated by NS5806, but for all subunit combinations tested, recovery was slowed by NS5806.

Besides the various ancillary subunits that have been implied to contribute to native I_{to}, other channel-forming subunits have also been suggested; for other species, including humans, K_V1.4 has been reported to contribute to I_{to} (Patel and Campbell, 2005). Previous studies have found K_V1.4 mRNA (Dixon *et al.*, 1996; Rosati *et al.*, 2001) and K_V1.4 protein (Akar *et al.*, 2004) in the canine left ventricle. However, the functional role of K_V1.4 and $I_{to,slow}$ in canine tissue is uncertain. Akar and colleagues found no appreciable contribution of K_V1.4 current to canine ventricular I_{to} (Akar *et al.*, 2004). Interestingly, for canine mid- and epicardial I_{to}, application of NS5806 accelerated the recovery but also changed the kinetics from bi-exponential to mono-exponential (Calloe *et al.*, 2009b). It was tempting to speculate whether this change in recovery kinetics could be due to enhancement of a fast recovering

current component in combination with inhibition of a slow recovering component of I_{to}. To test this hypothesis, the fast recovering $K_V4.3$/KChIP2/DPP6 channels were co-expressed with slowly recovering $K_V1.4$ channels in *Xenopus laevis* oocytes. The current generated by $K_V4.3$/KChIP2/DPP6/$K_V1.4$ recovered from inactivation with a bi-exponential time-course (Figure 8), similar to native I_{to}. In addition, NS5806 accelerated the recovery and changed the time-course from bi-exponential to mono-exponential. This suggests that $K_V1.4$ or some other slowly recovering current could contribute to native canine I_{to}. Whether this is the case *in vivo* remains to be determined. NS5806 slowed $K_V4.3$/KChIP2/DPP6/$K_V1.4$ current decay yet did not affect peak current amplitude. We consistently observed that NS5806 had little effect on amplitude of currents recorded in *Xenopus laevis* oocytes whereas current amplitudes were increased when similar constructs were expressed in CHO-K1 or HEK-293 cells (data not shown). Increasing the temperature to 37°C for the oocytes experiments and replacing the extracellular solution with that used for native I_{to} recordings did not alter the effect of NS5806 on $K_V4.3$/KChIP2 peak current amplitudes in *Xenopus laevis* oocytes (data not shown) suggesting that the observed difference was due to intrinsic differences between expression systems.

Comparison with other I_{to} affecting compounds

The effects of several compounds on $K_V4.3$ have been reported to be modulated by co-expression of ancillary subunits. The I_{Kr} blocker tedisamil inhibits $K_V4.3$/KChIP2 with different IC_{50} values depending on co-expression with KCNE1, KCNE2 or DPP6 due to differential modulation of current kinetics (Radicke *et al.*, 2009). Similarly for the class 1C anti-arrhythmic agent flecainide, the IC_{50} values for the peak current amplitudes of $K_V4.3$/KChIP2 are dependent on co-expression with KCNE1, KCNE2 or DPP6 (Radicke *et al.*, 2008). The inhibition of $K_V4.3$ current by the local anesthetic bupivacaine is reduced by co-expression of KChIP2 (Solth *et al.*, 2005). However, for these compounds the differences in drug action due to ancillary subunits are so subtle that they limit their usefulness to investigate the molecular constituents of native I_{to} or I_A channel complexes. The calcium channel blocker nifedipine is an open-pore blocker of $K_V4.3$ and $K_V4.3$/KChIP2 channels when used in high concentrations (150 μM). Interestingly, the time-dependent recovery of $K_V4.3$ is markedly slowed by nifedipine whereas in the presence of KChIP2 the recovery is unaffected by the compound (Bett *et al.*, 2006). This suggests that nifedipine can be used to identify the presence of KChIP2 in native channels; however, the effect on I_{CaL} may be an issue in some preparations. For NS5806, a small inhibiting effect on I_{CaL} and I_{Na} in isolated canine ventricular cells was observed (Calloe *et al.*, 2009a), and in the present work we found that NS5806 inhibits $K_V1.4$ and $K_V1.5$ currents. Nevertheless, even with these caveats in mind, NS5806 provides a tool to address the physiological role and the molecular composition of I_{to} and I_A.

Limitations of this study

In the present study we compared the effect of NS5806 on heterologously expressed putative human I_{to} channel subunits. The results were compared with results obtained in a previous paper where we characterized the effect of NS5806 on canine ventricular I_{to} (Calloe *et al.*, 2009b). Canine I_{to} has a faster current decay and recovers slower from inactivation than human I_{to}. Additionally, human I_{to} recovery follows a single exponential time course, whereas canine I_{to} follows a biexponential time course (Akar *et al.*, 2004). We cannot exclude the possibility that the observed discrepancies between the effect of NS5806 on the heterologously expressed channels in this study and native canine I_{to} are due to species differences. However, more importantly, the expression systems may lack important regulatory factors, additional ancillary subunits, etc. found in native cells and the molecular composition of the native I_{to} channel remains speculative. Further *Xenopus laevis* oocyte experiments were performed at room temperature which slows the kinetic parameters compared with currents measured at 37°C. However, for screening as well as for expression of multiple constructs, the oocytes are preferable to mammalian cell lines.

In conclusion, NS5806 activates native I_{to} and K_V4 channels heterologously expressed with KChIP2 in both *Xenopus laevis* oocytes and CHO-K1 cells. The differential effect of NS5806 in the absence and presence of KChIP2 suggests that NS5806 besides providing an experimental model of the Brugada syndrome can be used as a tool to address the physiological role of I_{to} and I_A and potentially to identify the molecular components of the channels mediating the currents *in vivo*; however, this should be tested by complementary approaches.

Acknowledgements

The authors wish to thank Dr Morten B. Thomsen for valuable discussion, Trine Christensen for technical assistance and NeuroSearch A/S Ballerup, Denmark for providing NS5806.

This work was supported by grants from the Danish Cardiovascular Research Academy (DaCRA) and the Danish Heart Foundation (AL), the Danish National Research Foundation (NS, SPO), The Novo Nordisk Foundation (TJ), The Lundbeck Foundation (TJ), Carlsberg Foundation (KC), the American Health Assistance Foundation to JMC.

Conflicts of Interest Morten Grunnet is employed by NeuroSearch A/S and Søren-Peter Olesen is a consultant to the company.

References

Akar FG, Wu RC, Deschenes I, Armoundas AA, Piacentino V, III, Houser SR *et al.* (2004). Phenotypic differences in transient outward K+ current of human and canine ventricular myocytes: insights into molecular composition of ventricular Ito. Am J Physiol Heart Circ Physiol 286: H602–H609.

Alexander SPH, Mathie A, Peters JA (2009). Guide to Receptors and Channels (GRAC). 4th edn. Br J Pharmacol 158 (Suppl. 1): S1–S254.

Amadi CC, Brust RD, Skerritt MR, Campbell DL (2007). Regulation of Kv4.3 closed state inactivation and recovery by extracellular potassium and intracellular KChIP2b. Channels (Austin) 1: 305–314.

An WF, Bowlby MR, Betty M, Cao J, Ling HP, Mendoza G *et al.* (2000). Modulation of A-type potassium channels by a family of calcium sensors. Nature 403: 553–556.

Bahring R, Boland LM, Varghese A, Gebauer M, Pongs O (2001). Kinetic analysis of open- and closed-state inactivation transitions in human Kv4.2 A-type potassium channels. J Physiol 535: 65–81.

Bett GC, Rasmusson RL (2008). Modification of K+ channel-drug interactions by ancillary subunits. J Physiol 586: 929–950.

Bett GC, Morales MJ, Strauss HC, Rasmusson RL (2006). KChIP2b modulates the affinity and use-dependent block of Kv4.3 by nifedipine. Biochem Biophys Res Commun 340: 1167–1177.

Brahmajothi MV, Campbell DL, Rasmusson RL, Morales MJ, Trimmer JS, Nerbonne JM *et al.* (1999). Distinct transient outward potassium current (Ito) phenotypes and distribution of fast-inactivating potassium channel alpha subunits in ferret left ventricular myocytes. J Gen Physiol 113: 581–600.

Calloe K, Cordeiro JM, Di Diego JM, Hansen RS, Grunnet M, Olesen SP *et al.* (2009a). A transient outward potassium current activator recapitulates the electrocardiographic manifestations of Brugada syndrome. Cardiovasc Res 81: 686–694.

Calloe K, Soltysinska E, Jespersen T, Lundby A, Antzelevitch C, Olesen SP *et al.* (2009b). Differential effects of the transient outward K(+) current activator NS5806 in the canine left ventricle. J Mol Cell Cardiol doi:10.1016/j.yjmcc.2009.07.017.

Callsen B, Isbrandt D, Sauter K, Hartmann LS, Pongs O, Bahring R (2005). Contribution of N- and C-terminal Kv4.2 channel domains to KChIP interaction [corrected]. J Physiol 568: 397–412.

Delpón E, Cordeiro JM, Núñez L, Bloch-Thomsen PE, Guerchicoff A, Pollevick GD *et al.* (2008). Functional effects of *KCNE3* mutation and its role in the development of Brugada syndrome. Circ Arrhythmia Electrophysiol 1: 209–218.

Deschenes I, Tomaselli GF (2002). Modulation of Kv4.3 current by accessory subunits. FEBS Lett 528: 183–188.

Diochot S, Drici MD, Moinier D, Fink M, Lazdunski M (1999). Effects of phrixotoxins on the Kv4 family of potassium channels and implications for the role of Ito1 in cardiac electrogenesis. Br J Pharmacol 126: 251–263.

Dixon EJ, Shi W, Wang H-S, McDonald C, Yu H, Wymore RS *et al.* (1996). Role of the Kv4.3 K+ channel in ventricular muscle. A molecular correlate for the transient outward current. Circ Res 79: 659–668.

Ebbinghaus J, Legros C, Nolting A, Guette C, Celerier ML, Pongs O *et al.* (2004). Modulation of Kv4.2 channels by a peptide isolated from the venom of the giant bird-eating tarantula Theraphosa leblondi. Toxicon 43: 923–932.

Hatano N, Ohya S, Muraki K, Giles W, Imaizumi Y (2003). Dihydropyridine Ca2+ channel antagonists and agonists block Kv4.2, Kv4.3 and Kv1.4 K+ channels expressed in HEK293 cells. Br J Pharmacol 139: 533–544.

Kaulin YA, De Santiago-Castillo JA, Rocha CA, Nadal MS, Rudy B, Covarrubias M (2009). The dipeptidyl-peptidase-like protein DPP6 determines the unitary conductance of neuronal Kv4.2 channels. J Neurosci 29: 3242–3251.

Lundby A, Olesen SP (2006). KCNE3 is an inhibitory subunit of the Kv4.3 potassium channel. Biochem Biophys Res Commun 346: 958–967.

Lundby A, Ravn LS, Svendsen JH, Hauns S, Olesen SP, Schmitt N (2008). KCNE3 mutation V17M identified in a patient with lone atrial fibrillation. Cell Physiol Biochem 21: 47–54.

Nadal MS, Ozaita A, Amarillo Y, Vega-Saenz de ME, Ma Y, Mo W *et al.* (2003). The CD26-related dipeptidyl aminopeptidase-like protein DPPX is a critical component of neuronal A-type K+ channels. Neuron 37: 449–461.

Patel SP, Campbell DL (2005). Transient outward potassium current, 'Ito', phenotypes in the mammalian left ventricle: underlying molecular, cellular and biophysical mechanisms. J Physiol 569: 7–39.

Pourrier M, Zicha S, Ehrlich J, Han W, Nattel S (2003). Canine ventricular KCNE2 expression resides predominantly in Purkinje fibers. Circ Res 93: 189–191.

Radicke S, Cotella D, Graf EM, Ravens U, Wettwer E (2005). Expression and function of dipeptidyl-aminopeptidase-like protein 6 as a putative

beta-subunit of human cardiac transient outward current encoded by Kv4.3. J Physiol 565: 751–756.

Radicke S, Cotella D, Graf EM, Banse U, Jost N, Varro A *et al.* (2006). Functional modulation of the transient outward current Ito by KCNE beta-subunits and regional distribution in human non-failing and failing hearts. Cardiovasc Res 71: 695–703.

Radicke S, Vaquero M, Caballero R, Gomez R, Nunez L, Tamargo J *et al.* (2008). Effects of MiRP1 and DPP6 beta-subunits on the blockade induced by flecainide of Kv4.3/KChIP2 channels. Br J Pharmacol 154: 774–786.

Radicke S, Cotella D, Sblattero D, Ravens U, Santoro C, Wettwer E (2009). The transmembrane beta-subunits KCNE1, KCNE2, and DPP6 modify pharmacological effects of the antiarrhythmic agent tedisamil on the transient outward current I (to). Naunyn Schmiedebergs Arch Pharmacol 379: 617–626.

Rosati B, Pan Z, Lypen S, Wang HS, Cohen I, Dixon JE *et al.* (2001). Regulation of KChIP2 potassium channel beta subunit gene expression underlies the gradient of transient outward current in canine and human ventricle. J Physiol 533: 119–125.

Rosati B, Grau F, Rodriguez S, Li H, Nerbonne JM, McKinnon D (2003). Concordant expression of KChIP2 mRNA, protein and transient outward current throughout the canine ventricle. J Physiol 548: 815–822.

Sanguinetti MC, Tristani-Firouzi M (2006). hERG potassium channels and cardiac arrhythmia. Nature 440: 463–469.

Sanguinetti MC, Johnson JH, Hammerland LG, Kelbaugh PR, Volkmann RA, Saccomano NA *et al.* (1997). Heteropodatoxins: peptides isolated from spider venom that block Kv4.2 potassium channels. Mol Pharmacol 51: 491–498.

Solth A, Siebrands CC, Friederich P (2005). Inhibition of Kv4.3/KChIP2.2 channels by bupivacaine and its modulation by the pore mutation Kv4.3V401I. Anesthesiology 103: 796–804.

Wang Z, Fermini B, Nattel S (1995). Effects of flecainide, quinidine, and 4-aminopyridine on transient outward and ultrarapid delayed rectifier currents in human atrial myocytes. J Pharmacol Exp Ther 272: 184–196.

Wettwer E, Amos GJ, Posival H, Ravens U (1994). Transient outward current in human ventricular myocytes of subepicardial and subendocardial origin. Circ Res 75: 473–482.

Zarayskiy VV, Balasubramanian G, Bondarenko VE, Morales MJ (2005). Heteropoda toxin 2 is a gating modifier toxin specific for voltage-gated K+ channels of the Kv4 family. Toxicon 45: 431–442.

Zhang M, Jiang M, Tseng GN (2001). minK-related peptide 1 associates with Kv4.2 and modulates its gating function: potential role as beta subunit of cardiac transient outward channel? Circ Res 88: 1012–1019.

Supporting information

Additional Supporting Information may be found in the online version of this article:

Figure S1 $K_V4.1$ with and without KChIP2 were expressed in *Xenopus laevis* oocytes. Currents were elicited by protocols shown in Figure 5 in the absence (black) and presence of 10 μM NS5806 (red). (A) Peak current amplitude as a function of voltage, $n = 5$. (B) Total charge movement evaluated as area under current trace during the first 150 ms after complete activation, $n = 5$. (C) Steady-state mid-inactivation. Current amplitudes at this step was normalized, plotted as a function of the pre-pulse potential and fitted to Boltzmann equation. For $K_V4.1$, $V_{1/2}$ was –61 ± 0.4 mV in the absence and –75 ± 0.8 mV in the presence of NS5806, $n = 5$. For $K_V4.1$/KChIP2, $V_{1/2}$ was –45 ± 0.2 mV in the absence and –59 ± 0.2 mV in the presence of NS5806, $n = 6$. (D) The time constant of recovery was determined by a two-pulse protocol. The peak current at the second pulse was normalized to the first pulse and the data points obtained were fit to a single exponential function. For $K_V4.1$, $\tau = 109 \pm 3$ ms in the absence and $\tau = 492 \pm 24$ ms in the presence of NS5806, $n = 6$. For $K_V4.1$/KChIP2, $\tau = 16.8 \pm 1.3$ ms in the absence and $\tau = 52.8 \pm 3.3$ ms in the presence of NS5806, $n = 5$.

Figure S2 $K_V4.2$ with and without KChIP2 were expressed in *Xenopus laevis* oocytes. Currents were elicited by protocols shown in Figure 5 in the absence (black) and presence of 10 μM NS5806 (red). (A) Peak current amplitude as a function of voltage, $n = 6$. (B) Total charge movement evaluated as area under current trace during the first 150 ms after complete activation, $n = 6$. (C) Steady-state mid-inactivation. Current amplitudes at this step was normalized, plotted as a function of the pre-pulse potential and fitted to Boltzmann equation, For $K_V4.2$, $V_{1/2}$ was –65 ± 0.5 mV in the absence and –76 ± 0.8 mV in the presence of NS5806, $n = 6$. For $K_V4.2$/KChIP2, $V_{1/2}$ was –57 ± 0.3 mV in the absence and –67 ± 0.4 mV in the presence of NS5806, $n = 10$. (D) The time constant of recovery was determined by a two-pulse protocol. The peak current at the second pulse was normalized to the first pulse and the data points obtained were fitted to a single exponential function. For $K_V4.2$, $\tau = 176 \pm 12$ ms in the absence and $\tau = 328 \pm 16$ ms in the presence of NS5806, $n = 5$. For $K_V4.2$/KChIP2, $\tau = 27.6 \pm 1.1$ ms in the absence and $\tau = 44.2 \pm 1.9$ ms in the presence of NS5806, $n = 10$.

Figure S3 $K_V11.1$ was expressed in *Xenopus laevis* oocytes. Currents were elicited from a holding potential of –80 mV by a series of steps from –80 to

+40 mV in 10 mV increments. Tails current were measured at –60 mV. Recordings were made in the absence (black) and presence of 10 μM NS5806 (red). (A) Representative currents of $n = 5$ (B) Steady-state current amplitude plotted as a function of voltage, $n = 5$. (C) Peak tail-current amplitude as a function of voltage, $n = 5$.

Figure S4 $K_V7.1$ was expressed in *Xenopus laevis* oocytes. Currents were elicited from a holding potential of –80 mV by a series of steps from –80 to +40 mV in 10 mV increments. Tails current were measured at –60 mV. Recordings were made in the absence (black) and presence of 10 μM NS5806 (red). (A) Representative currents of $n = 5$ (B) Peak-current amplitude as a function of voltage, $n = 5$.

Figure S5 $K_{ir}2.1$, 2.2 or 2.3 were expressed in *Xenopus laevis* oocytes. From a holding potential of 0 mV, currents were activated a ramp protocol from –120 mV to +50 mV. Recordings were made in the absence (black) and presence of 10 μM NS5806 (red). (A) Representative recordings of $K_{ir}2.1$, $n = 5$. (B) Representative recordings of $K_{ir}2.2$, $n = 5$. (C) Representative recordings of $K_{ir}2.3$, $n = 5$.

Figure S6 Time-dependent recovery from inactivation of $K_V1.4$ and $K_V4.3$/KChIP2 co-expressed with $K_V1.4$ in *Xenopus laevis* oocytes. The time constant of recovery was determined by a two-pulse protocol. The peak current at the second pulse was normalized to the first pulse and the data points obtained were fitted to a single exponential function before (black) and after application of 10 μM NS5806 (red). (A) Reactivation of $K_V1.4$ in the absence of NS5806 showed a bi-exponential time course with $\tau_1 = 286 \pm 125$ ms and $\tau_2 = 2055 \pm 798$ ms pre-exponential factors of 0.65 ± 0.12 and 0.35 ± 0.002 for controls. In the presence of NS5806 a mono-exponential function could be fitted to the data with $\tau = 11\,297 \pm 3945$ ms, $n = 5$. (B) $K_V4.3$/KChIP2 co-expressed with $K_V1.4$ followed a bi-exponential time course for reactivation with $\tau1 = 40 \pm 11$ms and $\tau2 = 1384 \pm 260$ ms with pre-exponential factors of 0.8 ± 0.05 and 0.2 ± 0.01 respectively. In the presence of NS5806, $\tau1 = 79 \pm 10$ ms and $\tau2 = 6906 \pm 1450$ ms with pre-exponential factors of 0.96 ± 1.4 and 0.04 ± 0.001, respectively, $n = 7$.

Please note: Wiley-Blackwell are not responsible for the content or functionality of any supporting materials supplied by the authors. Any queries (other than missing material) should be directed to the corresponding author for the article.